2021 IEEE 17th International Conference on Automation Science and Engineering (CASE)
August 23-27, 2021. Lyon, France

A Novel Geometric Calibration Method for Active Stereovision System

Jierui Liu, Xilong Liu, Zhiqiang Cao, *Senior Member, IEEE*, Zhonghui Li, Junzhi Yu, *Fellow, IEEE*

2021 IEEE 17th International Conference on Automation Science and Engineering (CASE) | 978-1-6654-1873-7/21/$31.00 ©2021 IEEE | DOI: 10.1109/CASE49439.2021.9551530

Abstract—**In this paper, a novel active stereovision calibration method is proposed to determine the time-varying extrinsic parameters of the cameras. This method mainly focuses on the rotation of cameras around the corresponding spatial axes with deviation. In the offline calibration, the installation matrices and baseline matrix are determined by introducing geometrical characteristics that represents the relationship of rotation axis and the transformation of camera rotation. On this basis, the extrinsic parameters can be updated online. The proposed method solves the problem where the spatial relationship between each camera and its rotation axis can be arbitrary, which has been verified by the simulations as well as tracking and measurement experiments on the developed active stereovision platform.**

I. Introduction

Stereovision has become essential for many applications, such as 3D reconstruction [1], autonomous driving [2] and visual navigation [3]. To carry these tasks, it is necessary to know the spatial relationship among cameras or extrinsic parameters, especially for stereovision with dynamic cameras, which is referred to active stereovision system.

The fixed binocular system [4][5] is the simplest form of stereovision, where its two cameras keep fixed spatial relationship with constant extrinsic parameters. Visual measurement can be achieved by employing the photography geometry and stereo matching. However, this type of system relies on the off-line calibrated parameters [6], which leads to limited measurement range. To overcome the problem above, active stereovision system [7][8][9] has been introduced, where two cameras can be adjusted dynamically. The active stereovision system is more flexible with a wider range by changing optic axes of cameras. Besides, the system can capture the object within center of the image, which avoids nonlinear distortion of camera lens and depth estimation is less sensitive to disparity. As a result, the precision of measurement is increased. A problem of active stereovision system is the calibration of extrinsic parameters, and the precision of calibration directly affects performance of measurement.

Conventional applications of stereovision usually consider the fixed stereovision system whose calibration is solved using Zhang's algorithm [10]. With the spreading of active vision, the aforementioned calibration solution becomes insufficient and the relative pose of cameras has to be taken into account. An online calibration way is to relocate the relative pose between cameras, which can estimate the extrinsic parameters online without requiring pre-calibration of the camera [9][11][12]. In [11][12], the relative pose is updated by local mapping and global optimization, which takes certain time to relocate the cameras, whereas Lins et al. [9] relocated the cameras using collaborative robots and each of which is equipped with a single camera. In order to acquire varying extrinsic parameters in real-time, more researchers adopt two-stage calibration method. The first stage calibrates mechanical parameters offline; on this basis, the second stage updates extrinsic parameters online. Das and Waslander [13] used the Denavit-Hartenberg convention to parametrize the actuated mechanism, which provides the basis to estimate the time-varying extrinsic transformations of cameras. Mohamed et al. [7] calibrated the relationship between the rotation angle in the image space and the platform space, which is used to update the extrinsic parameters online, however, the translation between the camera and the rotation axis is ignored.

In practice, some researches require the actuation mechanism to keep its rotating axis intersecting with the origin of the camera, which means that distance between the origin of each camera and corresponding rotation axis is expected to be small enough. However, the error caused by this distance is inevitable. Although this problem has been alleviated by careful mechanism designing [7][8][14], it is hard to manually adjust this distance to be zero. [13][15] go further, and the constraint between the rotating axis of the actuation mechanism and the camera's origin is released. How to better improve the accuracy of calibration requires further research.

In this paper, a novel active stereovision calibration method is proposed. Specially, geometrical characteristics to represent the relationship of rotation axis and the transformation of camera rotation are introduced. As a result, the problem where the spatial relationship between each camera and its rotation axis can be arbitrary is solved. On this basis, accurate extrinsic parameters are updated online.

The paper is organized as follows. Section II describes the related work. Problem statement is given in Section III. Section IV introduces the proposed calibration solution. The verifications are illustrated in Section V and Section VI concludes the paper.

This work is supported in part by the National Natural Science Foundation of China under Grants 61973302, 62073322, 61633020, Z191100008019004. (Corresponding author: Xilong Liu)

Jierui Liu, Xilong Liu, Zhiqiang Cao are with Institute of Automation, Chinese Academy of Sciences, Beijing 100190, China, and also with School of Artificial Intelligence, University of Chinese Academy of Sciences, Beijing 100049, China.

Zhonghui Li is with Beijing Engo Technology Co., Ltd, Beijing, China.

Junzhi Yu is with State Key Laboratory of Management and Control for Complex Systems, Institute of Automation, CAS, Beijing 100190, China, and also with State Key Laboratory for Turbulence and Complex System, Department of Mechanics and Engineering Science, BIC-ESAT, College of Engineering, Peking University, Beijing 100871, China.

II. Related Work

The methods based on re-localization calibrate the extrinsic parameters by relocating the relative positions between cameras and the reference camera [9][11][12]. Ince et al. [11] modeled the calibration as a re-localization problem and conducted multiple monocular SLAMs with only one loop closing thread. It initializes the relative pose between cameras and reference camera by solving Perspective-n-Point (PnP), and then carries out the tracking and local mapping. Zhang et al. [12] proposed an online calibration method based on feature descriptor for non-overlapping multi-camera system. It extracts the pose information for each image of feature descriptor-based calibration pattern and builds a complete map relative to the first camera. Then all the cameras are tracked in the same map and the extrinsic parameters can be obtained. Both of them [11][12] are suitable for the system where all the cameras are fixed. Some extra information is required to relocate their relative positions when their extrinsic parameters change. Lins et al. [9] used 24 infrared cameras to provide the information for pose estimation, which assists the re-location of cameras. These extra equipments increase the cost and the measurement accuracy subjects to the influence from the pose estimation. These methods do not concern the dynamic part of mechanism, which possibly reduces accuracy.

With consideration of mechanism, two-stage calibration receives much attention. The offline calibration procedure about mechanism is done firstly and then the extrinsic parameters are updated online, leading to the more accurate and faster online calibration. Grosso et al. [8] focused on the calibration of the motor angle offsets. The angular offsets of the encoders are compensated by manually measuring the vergence angles off-line for resetting the origin of the encoder counts. This is helpful to obtain the extrinsic parameters online. Kwon et al. [16] conducted the calibration by estimating the locations and the orientations of the rotating axes corresponding to the cameras through a closed-form solution. Sapiens et al. [17] introduced a calibration update procedure by an offline mapping from motor-based to image-based estimates of the camera orientations. Mohamed et al. [7][14] updated the extrinsic parameters of the system with two stages. The first is the offline calibration using [10], and the essential matrix describing the relative pose from the left image to the right image is obtained. Then, the rotation angle relationship between the image space and the platform space is acquired for the essential matrix in the rectification process of online calibration. However, it is required to keep rotating axis of the actuation mechanism intersecting with the origin of the camera, which means that the distance between the origin of each camera and corresponding rotation axis is expected to be small enough. However, it cannot be satisfied in some practical situations.

Some progresses have been achieved [13][15]. Wang et al. [15] used hand-eye calibration to calibrate the pose of each camera relative to the system, and the relative camera poses are obtained by combining the poses of each camera relative to the mechanical system. It has no strict limitation on the precision of camera installation, but it still assumed that the axes of multiple rotating shafts of the mechanical system are intersected, which decreases generalization. Das et al. [13] parameterized the actuated mechanism using the DH convention, which is calibrated using a fiducial marker of known scale. Thus, the distance restriction is released.

III. Problem Statement

This paper presents the calibration of active stereovision system with the change of yaw angles, where each camera can rotate around its rotation axis driven by a motor without translation.

We label as $\{C_1\}$ and $\{C_2\}$ the coordinate systems of left and right cameras, respectively. For each coordinate system, its origin is at the optical center of camera, its *z*-axis and *x*-axis are parallel to the optical axis and the *u*-axis of the image coordinate system. $\{L_1\}$ and $\{L_2\}$ are denoted as rotation axis coordinate systems, respectively, and each of which takes a point on the axis as the origin. Noted that the origin of $\{L_1\}$ or $\{L_2\}$ can be chosen arbitrarily, and the strict constraint of keeping rotating axis of the actuation mechanism intersecting with the camera's origin can be released. Fig. 1 illustrates the coordinate systems.

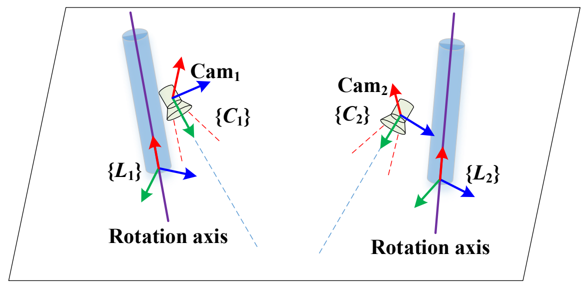

Fig. 1. Schematic diagram of coordinate system.

The pose matrix of the camera coordinate system in corresponding rotation axis coordinate system is given by:

$$\begin{cases} {}^{L_1}\mathrm{T}_{C_1} = Rot(y,\theta_1)\mathrm{T}_1 \\ {}^{L_2}\mathrm{T}_{C_2} = Rot(y,\theta_2)\mathrm{T}_2 \end{cases} \tag{1}$$

where ${}^{L_i}\mathrm{T}_{C_i} \in SE(3)$ represents the pose matrix corresponding to the i^{th} camera, $Rot(y,\theta_i)$ represents the posture transformation matrix of the rotation angle θ_i around the *y*-axis and *i*=1,2. T_i is the initial value of ${}^{L_i}\mathrm{T}_{C_i}$, which is determined by the mechanical design and installation error. $\mathrm{T}_i \in SE(3)$ is termed as the installation matrix of the i^{th} camera in this paper.

To represent the spatial relationship between Cam_1 and Cam_2, the pose transformation matrix ${}^{L_1}\mathrm{T}_{L_2} \in SE(3)$ between $\{L_1\}$ and $\{L_2\}$ is required, which is referred as baseline matrix. With T_1, T_2, θ_1, θ_2 and ${}^{L_1}\mathrm{T}_{L_2}$, the extrinsic parameters between Cam_1 and Cam_2 can be obtained, where θ_1 and θ_2 can be directly obtained from readings of motor encoders.

IV. The Proposed Calibration Method

The whole calibration process includes offline calibration of the installation matrices T_1, T_2 and the baseline matrix ${}^{L_1}\mathrm{T}_{L_2}$ as well as online updating of the extrinsic parameters of stereovision using the offline calibration results. Specially, the geometrical characteristics of rotation motion is additionally considered, and camera origin and its rotation axis can be decoupled.

To obtain the extrinsic parameters, the pose transformation matrix from Cam$_2$ to Cam$_1$ is as follows:

$$ {}^{C_1}\mathrm{T}_{C_2} = {}^{C_1}\mathrm{T}_{L_1}\,{}^{L_1}\mathrm{T}_{L_2}\,{}^{L_2}\mathrm{T}_{C_2} \tag{2} $$

Combining (1) and (2), the online updating of extrinsic parameters is given by

$$ {}^{C_1}\mathrm{T}_{C_2} = \mathrm{T}_1^{-1} Rot(y, -\theta_1)\,{}^{L_1}\mathrm{T}_{L_2} Rot(y, \theta_2)\mathrm{T}_2 \tag{3} $$

A. *Installation Matrix*

We label $\theta_{1,j}$ and $\theta_{2,j}$ as the rotation angles θ_1 and θ_2 at j^{th} sampling, where j=1, 2, ..., M. $\theta_{1,1}$ and $\theta_{2,1}$ correspond to the initial positions of Cam$_1$ and Cam$_2$. By visual measurement technology [10] (checkerboard calibration board is used), the poses $\mathrm{T}_{C_1}(\theta_{1,j})$ and $\mathrm{T}_{C_2}(\theta_{2,j})$ of Cam$_1$ and Cam$_2$ relative to respective initial position can be acquired. Obviously, $\mathrm{T}_{C_1}(\theta_{1,1}) = \mathrm{T}_{C_2}(\theta_{2,1}) = I$. According to the definition of the installation matrix, T_1 is given by

$$ \mathrm{T}_1 = {}^{L_1}\mathrm{T}_{C_1}(\theta_{1,1}) \tag{4} $$

Combining (4) with the transformation relationship ${}^{L1}\mathrm{T}_{C1} = Rot(y, -\theta_1)\mathrm{T}_1$ and $\mathrm{T}_{C_1}(\theta_{1,j}) = \left({}^{L_1}\mathrm{T}_{C_1}(\theta_{1,1})\right)^{-1}\,{}^{L_1}\mathrm{T}_{C_1}(\theta_{1,j})$, we have

$$ \mathrm{T}_{C_1}(\theta_{1,j}) = \mathrm{T}_1^{-1} Rot(y, -\theta_1)\mathrm{T}_1 \tag{5} $$

It is seen that each j corresponds a group of equations in terms of T_1. Multi-group equations with different j are combined to calculate T_1 [18]. For this solution, a problem is that the calibration of T_{C_1} at given rotation angle is sometimes not accurate enough. Besides, it is time-consuming. Actually, there exist inherent geometrical characteristics for camera rotation as follows:

1) The rotation axis of Cam$_1$ lies on the vertical bisector of the line segment represented by the translation part of $\mathrm{T}_{C_1}(\theta_{1,j})$, which means that the rotation axis of Cam$_1$ and the translation vector of $\mathrm{T}_{C_1}(\theta_{1,j})$ are orthogonal;
2) The rotation vector from the rotation of $\mathrm{T}_{C_1}(\theta_{1,j})$ is parallel to the rotation axis of Cam$_1$, and the vector norm is equal to the angle difference $\theta_{1,j} - \theta_{1,1}$ in a unit of radian.

Using the aforementioned characteristics, a novel geometric solution is proposed to solve (5). As a result, the installation matrix and the baseline matrix shall be calibrated with M=2.

As shown in Fig. 2, the process of rotating $\theta_{1,j}$ around the rotation axis of the camera from the initial position involves three coordinate systems $\{C_1(\theta_{1,1})\}$, $\{C_1(\theta_{1,j})\}$ and $\{L_1\}$, and O_1, O_2 denote the origins of the first two systems.

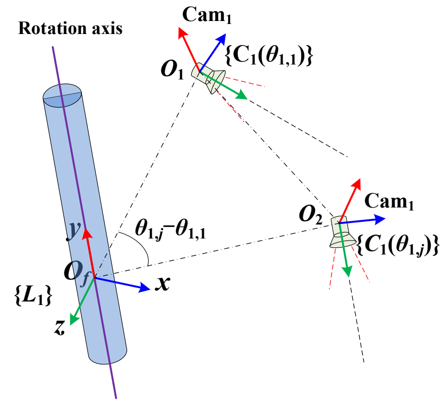

Fig. 2. Schematic diagram of different positions of a camera during the rotation of the axis.

With the line O_1O_2, we construct a plane $O_1O_2O_f$, which is orthogonal to the rotation axis, where O_f is the intersection of the plane and the rotation axis. With O_f being the origin and the rotation axis direction as the y axis, the axis coordinate system $\{L_1\}$ is represented. The pose matrix $\mathrm{T}_{C1}(\theta_{1,j})$ of $\{C_1(\theta_{1,j})\}$ in $\{C_1(\theta_{1,1})\}$ is known with its translation part is the vector $\overrightarrow{O_1O_2}$. Its rotating part is used to calculate the direction vector $\boldsymbol{f} = [f_a, f_b, f_c]^{\mathrm{T}}$ by Rodriguez formula, where $\boldsymbol{f}$ is consistent with the y-axis of $\{L_1\}$ in $\{\mathrm{C}_1(\theta_{1,1})\}$. In addition, according to the triangle constraint, the length l of $\overrightarrow{O_1O_f}$ can be obtained, and we have

$$ \begin{cases} \boldsymbol{f}\cdot\overrightarrow{O_1O_f} = 0 \\ \left\|O_1O_f\right\|_2^2 = l^2 \\ \left\|O_2O_f\right\|_2^2 = l^2 \end{cases} \tag{6} $$

Theoretically, the representation of O_f in $\{C_1(\theta_{1,1})\}$ can be solved by (6), however, it belongs to the second-order equations of 3 variables, which possibly generates several possible solutions due to the arbitrariness of O_1 and camera rotation axis. Although the right solution can be screened according to preset rules, it is trivial. An efficient scheme to acquire O_f is required.

With the combination of the coordinate of O_2 in $\{C_1(\theta_{1,1})\}$, the vertical bisector P$_1$ of the line segment O_1O_2 in $\{C_1(\theta_{1,1})\}$ is obtained. Then the intersection line between plane P$_1$ and plane $O_1O_2O_f$ is produced, and its direction vector is described as $\boldsymbol{r}$.

$$ \overrightarrow{O_1O_f} = \frac{1}{2}\overrightarrow{O_1O_2} + \boldsymbol{r} \tag{7} $$

where $\overrightarrow{O_1O_f}$ and $\overrightarrow{O_1O_2}$ refer to the vectors from O_1 to O_f and O_2, respectively. At this point, we get the representation of O_f in $\{C_1(\theta_{1,1})\}$, i.e., $\overrightarrow{O_1O_f}$.

TABLE I. THE RESULTS OF PROPOSED OFFLINE ESTIMATION FOR SIMULATION 1 (unit: mm)

	T_1 translation	T_2 translation	T_1 rotation direction	T_2 rotation direction	${}^{L1}T_{L2}$ translation	${}^{L1}T_{L2}$ rotation direction
Ground truth	(0.00,0.00,-40.00)	(0.00,0.00,-40.00)	(0.00,0.99,-0.02)	(0.00,0.99,-0.02)	(-199.24,0.00,17.43)	(0.00,1.00,0.00)
calibration	(-0.06,0.00,-40.09)	(-0.01,0.00,-40.11)	(0.00,0.99,-0.02)	(0.00,0.99,-0.02)	(-198.98,-0.30,17.27)	(0.00,1.00,0.00)

TABLE II. THE ERRORS OF THE EXTRINSIC PARAMETERS UPDATED ONLINE FOR SIMULATION 1

θ_1 (rad)	θ_2 (rad)	Translation error (mm)	Direction error of rotation vector (rad)	Rotation angle error (rad)
-0.7	0.5	0.548827	0.000908	0.000458
-0.3	0.5	0.528621	0.001093	0.000458
-0.5	0.3	0.548827	0.000908	0.000458
0.0	0.0	0.498068	0.003036	0.000458
0.5	-0.3	0.454208	0.000055	0.000458
0.3	-0.5	0.470447	0.000530	0.000459
0.5	-0.7	0.454208	0.000055	0.000458

As for the rotation part of ${}^{C_1}\mathrm{T}_{L_1}(\theta_{1,1})$, we have acquired its x-component $\frac{\overrightarrow{O_1O_f}}{\|\overrightarrow{O_1O_f}\|}$ and its y-component $\frac{\boldsymbol{f}}{\|\boldsymbol{f}\|}$. The remaining z-component $\boldsymbol{e_z}$ can be obtained by the right-hand theorem:

$$\boldsymbol{e_z} = \frac{\overrightarrow{O_1O_f}\times\boldsymbol{f}}{\|\overrightarrow{O_1O_f}\times\boldsymbol{f}\|} \tag{8}$$

Therefore, ${}^{C_1}\mathrm{T}_{L_1}(\theta_{1,1})$ can be written as:

$${}^{C_1}\mathrm{T}_{L_1}(\theta_{1,1}) = \begin{bmatrix} \frac{\overrightarrow{O_1O_f}}{\|\overrightarrow{O_1O_f}\|} & \frac{\boldsymbol{f}}{\|\boldsymbol{f}\|} & \boldsymbol{e_z} & \overrightarrow{O_1O_f} \\ & \boldsymbol{0} & & 1 \end{bmatrix} \tag{9}$$

Combining (4) and (9), we get the installation matrix T_1 as follows:

$$\mathrm{T}_1 = \left({}^{C_1}\mathrm{T}_{L_1}(\theta_{1,1})\right)^{-1} \tag{10}$$

Similarly, the installation matrix T_2 is acquired.

B. Baseline Matrix

Through stereo calibration based on overlapping field of view, the extrinsic parameters matrix ${}^{C_1}\mathrm{T}_{C_2}(\theta_{1,1},\theta_{2,1})$ in the initial state is obtained by setting $\theta_{1,1}=\theta_{2,1}=0$ and $Rot(y,-\theta_1)=Rot(y,\theta_2)=I$. Utilizing equation (3), the baseline matrix ${}^{L_1}\mathrm{T}_{L_2}$ is as follows:

$${}^{L_1}\mathrm{T}_{L_2} = \mathrm{T}_1\,{}^{C_1}\mathrm{T}_{C_2}(\theta_{1,1},\theta_{2,1})\mathrm{T}_2^{-1} \tag{11}$$

V. VERIFICATIONS

In this part, the proposed calibration method is evaluated on both simulation and experiment.

A. Simulation

A simulation system is developed, which takes the information of extrinsic and intrinsic parameters of two virtual cameras as well as the spatial information of fiducial marker as input, and outputs the synthetic image from cameras. The simulation system allows us to obtain the ground truth of parameters requiring being calibrated. We model the pinhole camera with the length and width of image and intrinsic matrix:

$$K = \begin{bmatrix} f_x & 0 & c_x \\ 0 & f_y & c_y \\ 0 & 0 & 1 \end{bmatrix} \tag{12}$$

where K assumes that the cameras do not generate any distortion, f_x and f_y denote the scales from camera coordinate system to the image coordinate, c_x and c_y refer to the bias of the camera origin in the image.

For virtual Cam_1 and Cam_2, the rotation axes are modeled by the installation matrices T_1 and T_2, which are fixed during the rotation motion. The baseline matrix ${}^{L_1}\mathrm{T}_{L_2}$ of the rotation axis coordinate systems $\{L_1\}$ and $\{L_2\}$ connects two rotation axes, which make Cam_1 and Cam_2 an active binocular system.

We consider two simulations, where the distance between the origins of $\{L_1\}$ and $\{L_2\}$ is 200mm and there inevitably exist little drift angle between the y-axis of cameras and the rotation axes. Simulation 1 sets a larger distance 40mm between the origin of each camera and corresponding rotation axis, whereas this distance is only 1mm in simulation 2, which simulate the situation the deviation between the camera origin and rotation axis while it is not supposed to exist ideally.

The results of simulation 1 are given in Tables I and II. Table I describes the results of proposed offline calibration about T_1, T_2 and ${}^{L_1}\mathrm{T}_{L_2}$. Table II shows the errors of the extrinsic parameters updated online. One can see that our calibration method achieves submillimeter accuracy, especially the error of installation matrices is less than 0.20mm. Besides, the extrinsic parameters updated online are very close to the Ground truth based on the precise calibration of offline parameters. Tables III and IV describe the results of simulation 2 which have the similar conclusion as simulation 1. In Table IV, the methods of [7] and [13] are also presented, where we limit the rotation angle of each camera to 20° when calibrating offline to always hold the marker in the image. Note that the accuracy of [13] can be further increased when the limitation of camera movement is loosen. It is seen from Table IV that our method achieves comparable result.

B. Experiment

We develop an active stereovision platform for dynamic tracking and measurement experiments, as illustrated in Fig. 3. The platform consists of 2 Baumer HXC13 cameras whose resolution is 1280×1024, and each of them can rotate around its rotation axis driven by motors independently. The origins of cameras are far from the rotation axis, which could reach

TABLE III. THE RESULTS OF PROPOSED OFFLINE ESTIMATION FOR SIMULATION 2 (unit: mm)

	T_1 translation	T_2 translation	T_1 rotation direction	T_2 rotation direction	${}^{L1}T_{L2}$ translation	${}^{L1}T_{L2}$ rotation direction
ground truth	(0.00,0.00,-1.00)	(0.00,0.00,-1.00)	(0.00,0.99,-0.09)	(0.00,0.99,-0.09)	(-199.24,0.00,17.43)	(0.00,1.00,0.00)
calibration	(-0.11,0.00,-1.02)	(-0.01,0.00,-1.17)	(0.00,0.99,-0.09)	(0.00,0.99,-0.09)	(-198.91,-0.20,17.24)	(0.00,1.00,0.00)

TABLE IV. COMPARISON OF DIFFERENT METHODS IN TERM OF TRANSLATION ERROR OF EXTRINSIC PARAMETERS UPDATED ONLINE FOR SIMULATION 2 (unit: mm)

θ_1 (rad)	θ_2 (rad)	[13]	[7]	our method
-0.7	0.5	2.698074	0.826349	0.468009
-0.3	0.5	1.942352	0.523360	0.437226
-0.5	0.3	2.698074	0.826349	0.548827
0.0	0.0	0.807555	0.392971	0.387800
0.5	-0.3	1.694930	1.193021	0.348338
0.3	-0.5	0.945361	0.835782	0.366271
0.5	-0.7	1.694930	1.193021	0.348338

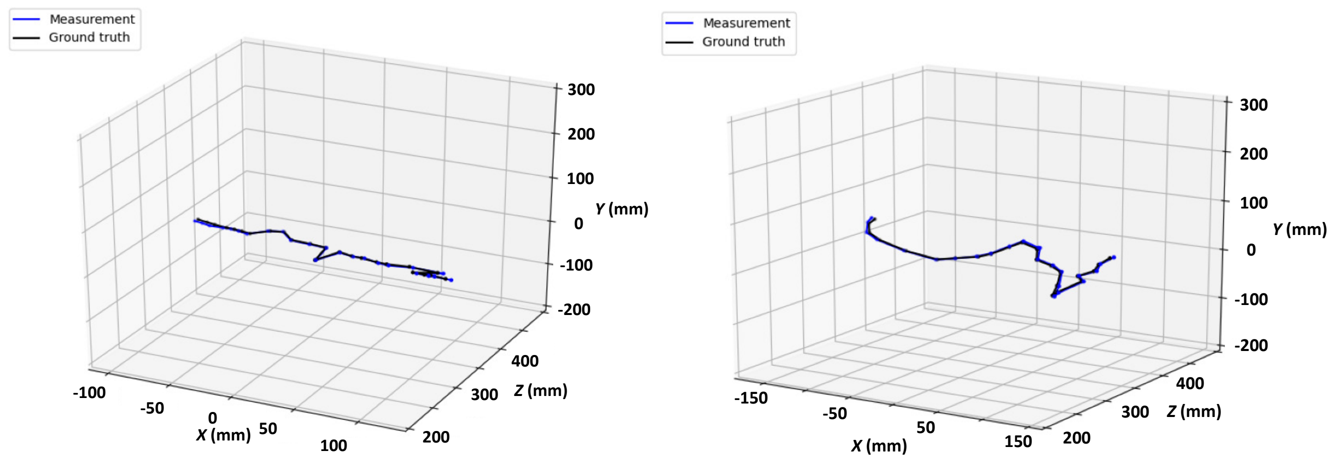

(a) (b)

Fig. 4. The trajectories of marker measured by stereovision platform. (a) the marker moves in a plane; (b) the marker moves in 3D space.

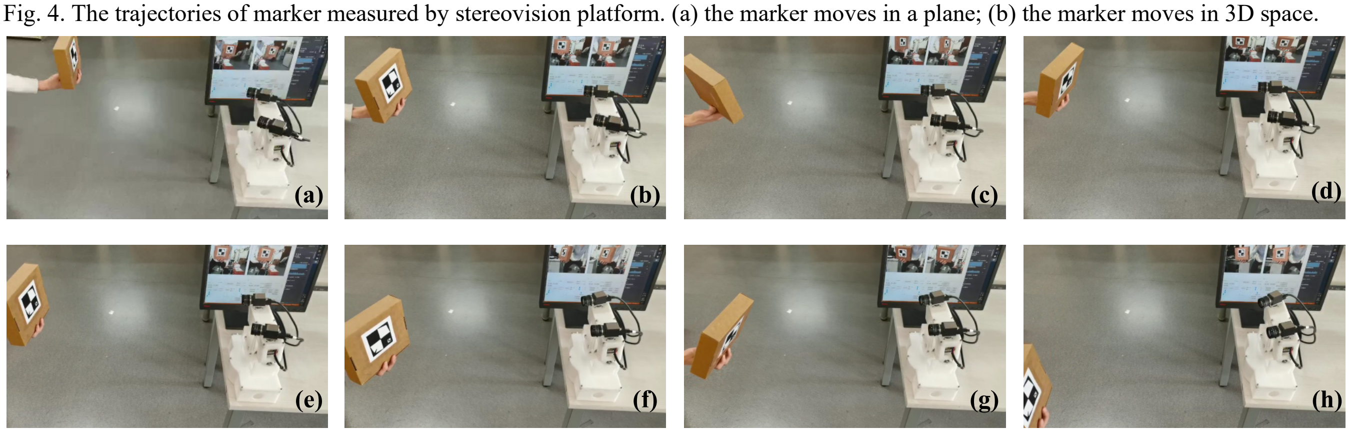

Fig. 5. The snapshots of experiment 1, where the marker moves from left to right with rotation.

about 42mm, and the rotation axis is not parallel to *y*-axis of any camera.

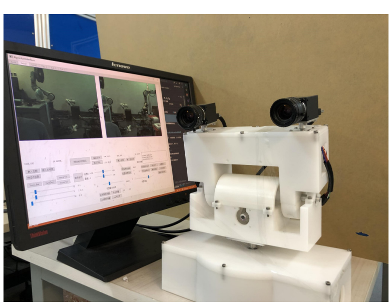

Fig. 3. Active stereovision platform.

With the results T_1, T_2 and ${}^{L1}T_{L_2}$ of offline calibration, tracking and measurement can be executed by adjusting the mechanism and updating the extrinsic parameters in real-time, where θ_1 and θ_2 are directly obtained from readings of motor encoders. To obtain the Ground truth trajectory of the object being tracked, we choose a mark as the object to be gazed and get its coordinates by solving PnP as Ground truth. The system tracks the object with visual servo and measures real-time world coordinate of the object by trigonometric survey with the extrinsic parameters updated online.

Fig. 4 presents the trajectories of the marker measured by active stereovision platform. We consider the planar and 3D motions of the handheld marker, and the results with 24

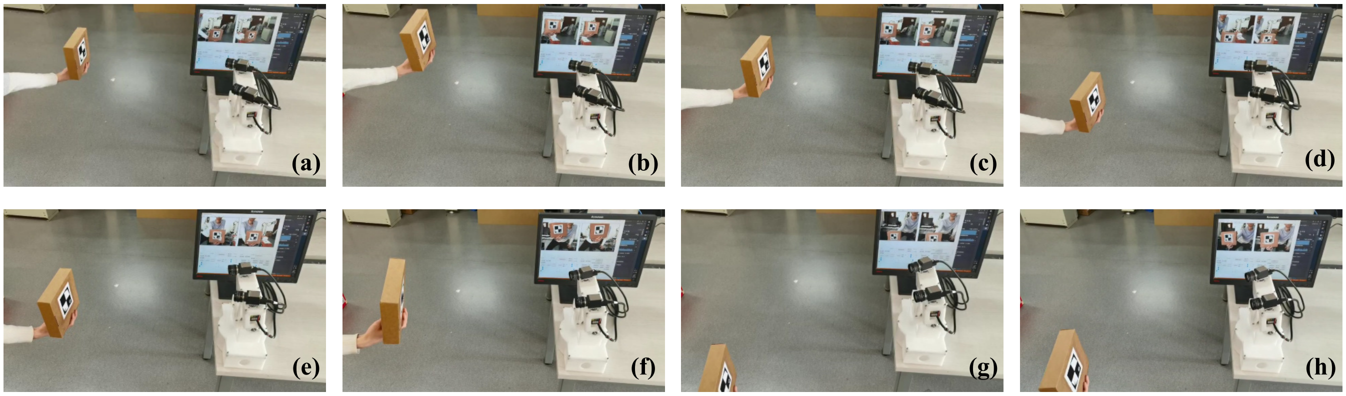

Fig. 6. The snapshots of experiment 2, where the marker moves from left to right with up and down fluctuation.

sampling points are given Figs. 4(a) and 4(b), respectively. It is seen that the mean errors of measurement with our method are small: 2.77mm and 2.56mm for Figs. 4(a) and 4(b). With the extrinsic parameters updated online, the vision system achieves gazing at the marker successfully, and the experiment snapshots are given in Fig. 5 and Fig. 6. The first experiment sets the marker to move from left to right in a plane with rotation, and the second one concerns the marker with up and down fluctuant motion. The results indicate that the vision system can adapt to the varying poses of the marker.

VI. Conclusion

This paper presents a calibration method based on geometrical characteristics for active stereovision system. By considering the relationship of rotation axis and the transformation of camera rotation, the system can handle the case, where the spatial relationship between each camera and its rotation axis is arbitrary. After the installation matrices and baseline matrix are calibrated offline, the extrinsic parameters can be updated online, which are used to measure the spatial coordinates of marker. The simulations and experiments prove the effectiveness of our vision system.

References

[1] P. Binh, Q. Nguyen. A review of stereo-photogrammetry method for 3-D reconstruction in computer vision. *19th International Symposium on Communications and Information Technologies*, Ho Chi Minh City, Vietnam, 2019: 138-143.

[2] L. Wang, Y. Wang, et al. Overview of environmental perception for intelligent vehicle. *IEEE Transactions on Intelligent Transportation Systems*, 2017, 18(10): 2584-2601.

[3] M. Burri, H. Oleynikova, M. W. Achtelik, R. Siegwart. Realtime visual-inertial mapping, re-localization and planning onboard MAVs in unknown environment. *IEEE/RSJ International Conference on Intelligent Robots and Systems*, Hamburg, Germany, 2015: 1872-1878.

[4] S. Kuindersma, R. Deits, M. Fallon, et al. Optimization-Based Locomotion Planning, Estimation, and Control Design for the Atlas Humanoid Robot. *Autonomous Robots*, 2016, 40(3): 429-455.

[5] K. Kaneko, K. Harada, F. Kanehiro, et al. Humanoid Robot HRP-3. *IEEE/RSJ International Conference on Intel-ligent Robots and Systems,* Washington, Nice, France, 2008: 2471-2478.

[6] P. Li, Y. Zhang. Global localization for indoor mobile robot based on binocular vision. *Laser & Optoelectronics Progress*, 2020, 28(4): 504-509

[7] A. Mohamed, P. Culverhouse, A. Cangelosi, et al. Active stereo platform: online epipolar geometry update. *Eurasip Journal on Image and Video Processing*, 2018:1-16.

[8] E. Grosso, M. Tistarelli. Active dynamic stereo vision. *IEEE Transactions on Pattern Analysis and Machine Intelligence*, 1995, 17(9): 868-879.

[9] R. G. Lins, S. N. Givigi, P. R. G. Kurka. Vision-based measurement for localization of objects in 3-D for robotic applications. *IEEE Transactions on Instrumentation and Measurement*, 2015, 64(4): 2950-2958.

[10] Z. Zhang. A flexible new technique for camera calibration. *IEEE Transactions on Pattern Analysis and Machine Intelligence*, 2000, 22(4): 1330-1334.

[11] O. F. Ince, J. Kim. Accurate On-line Extrinsic Calibration for a Multi-camera SLAM System. *International Conference on Ubiquitous Robots*, Japan, 2020: 540-545.

[12] L. Zhang, J. Zhang, et al. An Online Automatic Calibration Method Based on Feature Descriptor for Non-Overlapping Multi-Camera Systems. IEEE International Conference on Robotics and Biomimetics, Malaysia, 2018: 138-143.

[13] A. Das, S. L. Waslander. Calibration of a dynamic camera cluster for multi-camera visual SLAM. *IEEE/RSJ International Conference on Intelligent Robots and Systems*, Daejeon, 2016: 4637-4642.

[14] A. Mohamed, P. F. Culverhouse, et al. Automating Active Stereo Vision Calibration Process with Cobots. *International Federation of Automatic Control*. 2017, 50(2): 163-168.

[15] Q. Wang, W. Zou, F. Zhang, D. Xu. Binocular initial location and extrinsic parameters real-time calculation for bionic eye system. *Proceedings of the 11th World Congress on Intelligent Control and Automation*, China, 2014: 74-80.

[16] H. Kwon, J. Park, A. C. Kak. A new approach for active stereo camera calibration. *IEEE International Conference on Robotics and Automation*, Italy, 2007: 3180-3185.

[17] M. Sapienza, M. Hansard and R. Horaud. Real-time visuomotor update of an active binocular head, *Autonomous Robots*, 2012, 34: 35-45.

[18] Y. I. Abdel-Aziz, H. M. Karara, M. Hauck. Direct linear transformation from comparator coordinates into object space coordinates in close-range photogrammetry. *Photogrammetric Engineering and Remote Sensing*, 2015, 81(2): 103-107.